

## Study of Ce Promoter on Nano Structure Iron Catalyst in Fischer-Tropsch Synthesis

Yahya Zamani<sup>\*a,b</sup>, Mehdi Bakavoli<sup>b</sup>, Mohamad Rahimizadeh<sup>b</sup>, Ali Mohajeri<sup>a</sup>,  
Seyed Mohamad Seyedi<sup>b</sup>

<sup>a</sup> Gas Research division, Research Institute of Petroleum Industry (RIPI), National Iranian Oil Company; West Blvd., Near Azadi Sports Complex P.O. BOX 14665-137, Tehran, Iran

<sup>b</sup> Department of Chemistry, Ferdowsi University of Mashad, Azadi Square, Mashad, P.O. BOX 91735-48974, Iran  
[zamaniy@ripi.ir](mailto:zamaniy@ripi.ir)

Fischer–Tropsch synthesis (FTS) is an established technological route for upgrading natural gas, coal, and biomass to liquid fuels and other chemical products. Fe and Co catalysts are currently used in industrial scale. Effect of cerium element has been scrutinized on conventional nano-structure iron catalyst in FTS process. The nano-sized iron catalysts prepared by micro-emulsion method have composition in terms of atomic ratio as: 100Fe/3Cu, 100Fe/3Cu/ 1.5Ce, 100Fe/3Cu/ 3Ce. XRD, BET, TEM, and TPR techniques were utilized to assess the catalyst phases, structure, and morphology. The results indicated that promoted catalyst compare to the unpromoted catalyst, has higher FT rate and secondary reaction for CO<sub>2</sub> production but lower gas fraction.

### 1. Introduction

Fischer–Tropsch synthesis (FTS) has been used since the early 20th century to produce transportation fuels and chemicals from coal, natural gas and other C-based materials (Anderson et al., 1984, Bayat et al., 2010). Fischer–Tropsch Synthesis mechanisms was studied for iron catalysts (Davis, 2009). Intrinsic kinetics of Fischer–Tropsch Synthesis and water gas shift reactions over a precipitated iron catalyst were investigated (Van Der Laan and Beenackers, 2000). Iron-based catalysts are usually used for FTS due to their low cost, flexible product distribution and high FTS activity as well as high water-gas shift (WGS) activity (Pour et al., 2012; Pendyala et al., 2010). Among promoters, potassium has been used widely as a promoter for iron-based catalysts. It provides an increase in the alkene yield and a decrease in the fraction of produced CH<sub>4</sub> (Bukur et al., 1990, Luo et al., 2003). A positive affect of transition metals such as La, Mo, Ta, V, and Zr for FTS and WGS activities has also been reported (Zhao et al., 2009; Feyzi et al., 2011; Palma et al., 2011; Suo et al., 2012). Although the studies on the Fe-based FT catalysts are extensive, these are little reports for the effect of cerium promoter on nano-sized iron catalyst activity, so it seems to be necessary to conduct more studies in this field. In this study, a micro-emulsion method has been applied to prepare the three different Fe catalysts in order to investigate the effects of cerium on catalyst morphology, activity, and product selectivity in Fischer–Tropsch Synthesis. The catalysts were tested in a fixed-bed stainless steel reactor at FTS conditions.

### Experimental

#### 1.1 Catalyst Preparation

Nano-structure iron catalysts were prepared by water-in-oil microemulsion method. A water solution of metal precursors, FeCl<sub>3</sub>·6H<sub>2</sub>O was added to a mixture of an oil phase containing 1-butanol and

chloroform with a ratio of 1 : 1 and sodium dodecyl sulfate (SDS) as a surfactant. Sodium hydroxide in the aqueous phase was added as precipitating agent and stirred for 4 hours. The obtained mixture was left aside to decant overnight. The solid was recovered by centrifugation and washed thoroughly with distilled water and acetone. Finally, the samples were dried overnight at 120 °C, and subsequently calcined in air at 350 °C for 4 h. Nanostructure copper oxide and cerium oxide were prepared by the method which used for nanostructured iron oxide. At the next step, they were mixed together. The promoted catalysts were dried at 120 °C for 24 h and calcined at 350 °C for 4 h in air. All samples were pressed into pellets, crushed, and sieved.

### 1.2 Catalyst characterization

BET surface area and pore volume were determined by N<sub>2</sub> physisorption using a Micromeritics ASAP 2010 automated system. Average particle size of the calcined powders was measured by LEO 912AB TEM. XRD spectra of fresh catalyst were conducted with a Philips PW1840 X-ray diffractometer with monochromatized Cu (K $\alpha$ ) radiation for determining of iron phases. Temperature programmed reduction (TPR) profiles of the calcined catalysts were recorded using a Micromeritics TPD-TPR 290 system. The composition of catalysts was determined using atomic absorption instrument (perkin-elmer model 2380).

### 1.3 Reactor system and operation procedure

As shown in Figure.1, the catalytic reaction experiments were conducted in a fixed-bed stainless steel reactor. 1.2 g catalyst was loaded in a fixed-bed stainless steel reactor then activated by H<sub>2</sub> gas mixture with GHSV=3 nl.h<sup>-1</sup>.g.cat<sup>-1</sup> at atmospheric pressure with increasing temperature from ambient to 350 °C at 5 °C/min which is maintained for 16 h and then reduced to 270 °C. Activation is followed by the synthesis gas stream with H<sub>2</sub>/CO=1 and GHSV= 2 nl.h<sup>-1</sup>.g.Cat<sup>-1</sup> for 24 h in atmospheric pressure and 270 °C. After activation, the catalyst activity tests were performed at 290 °C, 1.7 MPa reaction pressure, H<sub>2</sub>/CO= 1 and GHSV=3 nl.h<sup>-1</sup>.g.Cat<sup>-1</sup>. The products were analyzed by a gas chromatograph Varian CP 3800 (Pour et al. ,2008 , Zamani et al.,2010).

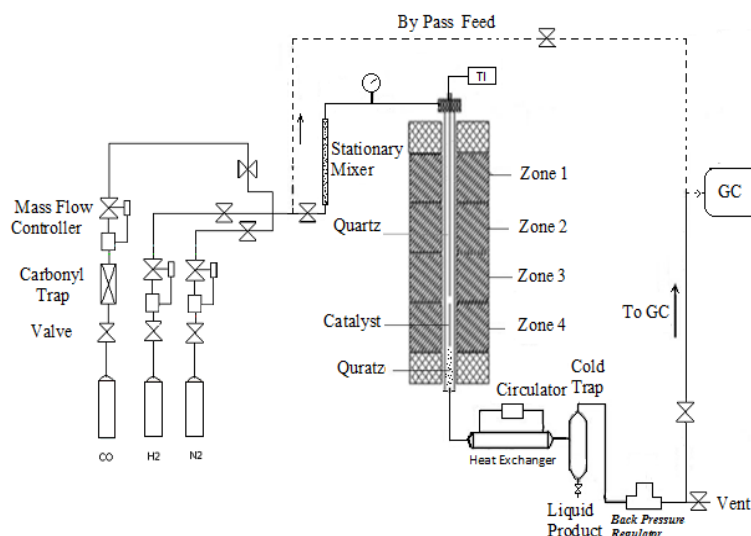


Figure 1: Cata - test system

## 2. Results and Discussion

Alkaline elements are used as promoters because they can modify the adsorption pattern of the reactants (H<sub>2</sub> and CO) on the active sites. The overall effects of these promoters as potassium on the behavior of the iron-based FTS catalysts; namely, CO chemisorptions enhancement has been justified as a consequence of the iron tendency to withdraw electronic density from potassium. Therefore, the

strength of the Fe–CO bond was enhanced (Herranz et al., 2006). At higher amount of alkali elements, CO dissociation proceeds faster than carbon hydrogenation. Therefore, it produces an excessive amount of carbon deposition and consequently deactivates the catalyst surface. Elemental analysis was performed to determine the composition of elements in the nano-sized catalysts. Three catalysts were prepared as 100Fe/3Cu, 100Fe/3Cu/1.5Ce, 100Fe/3Cu/3 Ce. Table.1 shows the result of textural properties of the catalysts. By adding of Cerium, the BET surface area and pore volume decrease when Cerium are combined to conventional catalyst. Furthermore, it promotes the aggregation of the catalyst crystallites and blocks up the pore volume.

Table 1. Textural properties of the catalysts

Catalysts	BET surface area (m <sup>2</sup> /g)	Pore volume (cm <sup>3</sup> /g)	Particle size d <sub>TEM</sub> (nm)	Particle size d <sub>XRD</sub> ( nm)
100Fe/3Cu	50.2	0.28	23.4	24.1
100Fe/3Cu/1.5Ce	48.6	0.26	24.4	24.2
100Fe/3Cu/3 Ce	47.4	0.25	25.1	24.9

The catalysts were characterized by X-ray diffraction (XRD) after calcinations. Figure. 2 shows the XRD patterns of the prepared catalyst. As shown in this figure, a new phase was not detected when Ce element was added. All the catalysts showed cubic hematite structured Fe<sub>2</sub>O<sub>3</sub> crystal according to JCPDS database. The characteristic peak at  $2\theta = 33.3^\circ$  corresponds to the hematite 104 plane and was used to calculate the average metal particle size by the Scherrer equation (Patterson A. ,1939).

The particle sizes of samples determined by XRD are summarized in Table 1. In general, particle sizes estimated from different techniques can provide different physical meanings. The XRD particle size (d<sub>XRD</sub>) obtained from XRD pattern indicates the average particle size. In addition, the average particle size can also be obtained by the Scherrer equation (eq.1) from broadening of the peaks in a wide angle X-ray scattering (WAXS) measurement of the material:

$$d = \frac{k\lambda}{\beta(\theta)\cos(\theta)} \quad (1)$$

Where  $\lambda$  is the X-ray wavelength (nm),  $\beta(\theta)$  the full width at half maximum (rad) of the identification peak,  $\theta$  is the diffraction angle and  $k$  is the typical constant of the equipment.

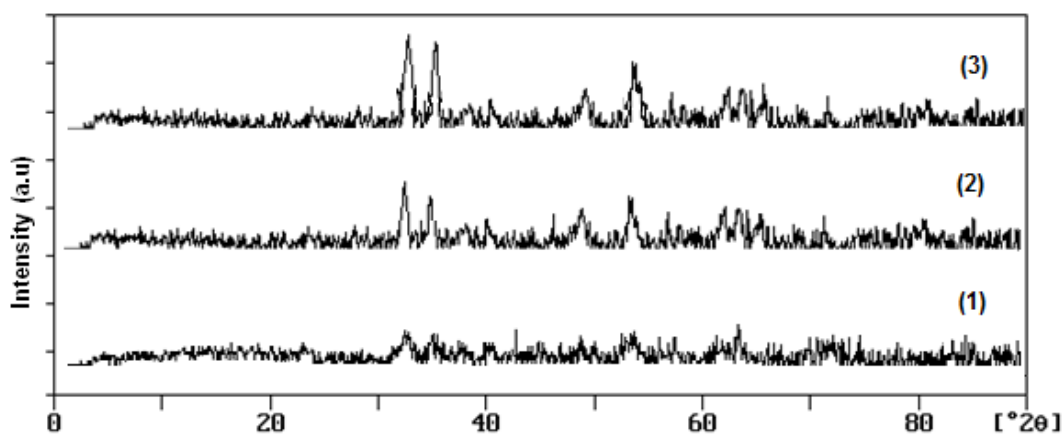
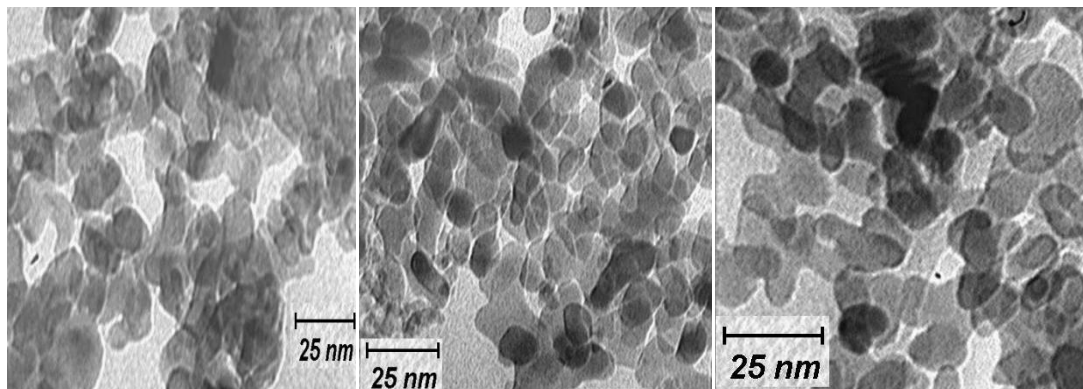


Figure 2: XRD spectra of the fresh catalysts: (1) 100Fe/3Cu (2) 100Fe/3Cu/1.5Ce (3) 100Fe/3Cu/3Ce

The morphology of catalysts was illustrated by TEM images in Figure 3. Although TEM revealed that the nanoparticles diameter was in the range of 20-30 nm, no distinguished difference was observed.



1)100Fe/3Cu

2)100Fe/3Cu/1.5Ce

3) 100Fe/3Cu/3Ce

Figure 3: TEM micrograph of the catalysts

Figure 4 shows the H<sub>2</sub>-TPR profiles of the catalysts. H<sub>2</sub>-TPR determined reduction behavior of the catalysts. The first stage is ascribed to the transformations of CuO to Cu, the second stage is attributed to the transformation of Fe<sub>2</sub>O<sub>3</sub> to Fe<sub>3</sub>O<sub>4</sub> whereas the third stage represents the transformation of Fe<sub>3</sub>O<sub>4</sub> to Fe. It is well known that CuO is easily reduced at lower temperature in H<sub>2</sub> atmosphere.

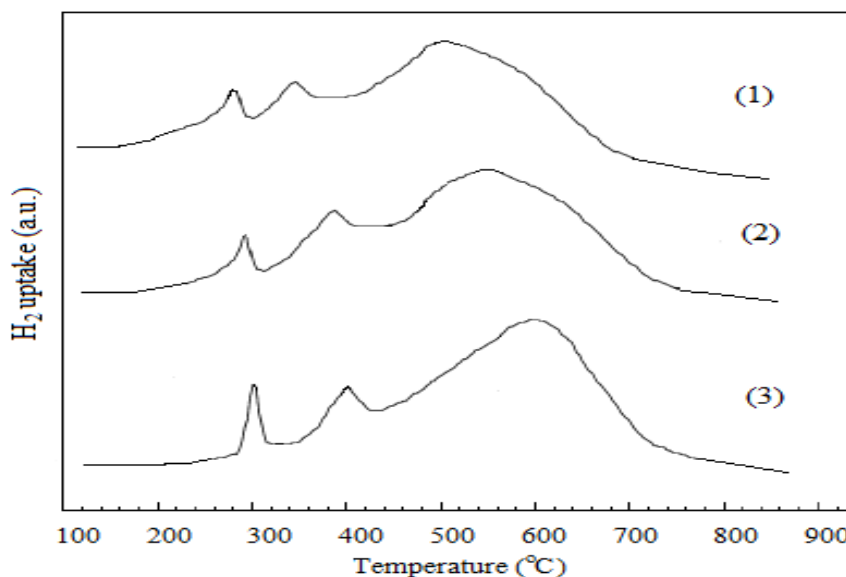


Figure 4: H<sub>2</sub>-TPR profiles of the catalysts

(1) 100Fe/3Cu (2) 100Fe/3Cu/1.5Ce (3) 100Fe/3Cu/3Ce

The addition of Cerium as promoter, apparently, improve the FTS activity of iron-based catalysts. However, promoted iron catalysts have higher FTS and WGS than unpromoted catalyst. Figure.5 shows FTS and WGS rates. During FTS process, part of produced water from FTS reaction is consumed by WGS reaction.

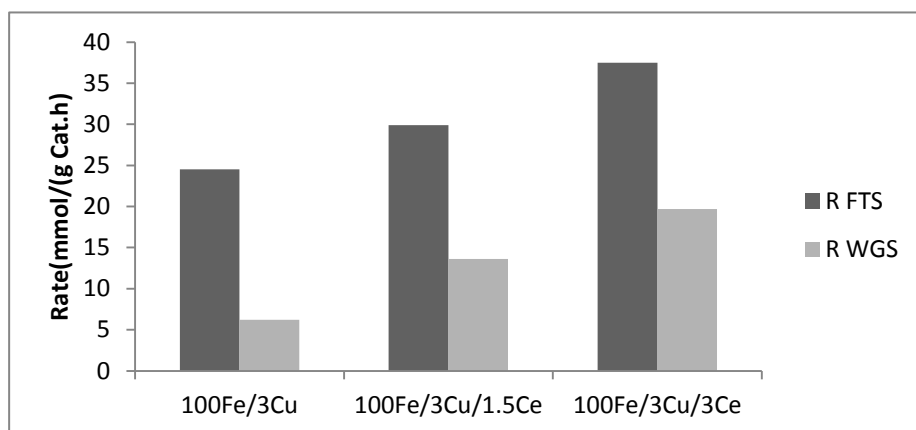


Figure 5:  $R_{FTS}$  and  $R_{WGS}$  of the catalysts

The incorporation of cerium as a promoter into iron-based catalyst can promote CO adsorption and concentration of CO species, and shift WGS reaction to right to improve WGS activity. Products selectivity are indicated in Table 2. It shows selectivities to gaseous and light hydrocarbons (methane and  $C_2-C_4$ ) and heavy hydrocarbons ( $C_5^+$ ). All of these results imply that the chain growth reaction is increased and the hydrogenation reaction is decreased while the promoter was added into the catalyst. Both the amount of the promoters and the reaction conditions influence the products selectivity. The mole fractions of hydrocarbons are obtained by the Anderson–Schulz–Flory (ASF) equation (Yang et al., 2004) as a function of the carbon number  $i$  and the chain growth probability  $\alpha$  (Eq.2):

$$x_i = (1 - \alpha) \alpha^{i-1} \quad (2)$$

Table 2. The activity and selectivity of the catalysts

Catalysts	100Fe/3Cu	100Fe/3Cu/1.5Ce	100 Fe/3Cu/3Ce
CO Conversion (%)	57.6	63.6	74.6
Products Selectivity (%mol)			
CH <sub>4</sub>	16.3	13.2	10.1
C <sub>2</sub> -C <sub>4</sub>	33.4	27.2	23.3
C <sub>5</sub> -C <sub>12</sub>	14.8	21.6	25.1
C <sub>13</sub> -C <sub>19</sub>	9.8	10.6	11.2
C <sub>19</sub> <sup>+</sup>	7.5	7.3	6.8
CO <sub>2</sub> <sup>a</sup> selectivity (%)	18.2	20.1	23.3
$\alpha^b$	0.61	0.65	0.72

Reaction condition: Time on Stream 72 h, 290 °C, 1.7MPa, H<sub>2</sub>/CO = 1.1 and SV= 3 nl.gCat<sup>-1</sup>. h<sup>-1</sup>.

<sup>a</sup> Selectivity to oxygenates was negligible (<3 %) in all cases

<sup>b</sup>  $\alpha$  = Chain Growth Probability

The results indicated that in comparison to the unpromoted catalyst, the promoted catalyst enhanced FT rate and secondary reaction rate for CO<sub>2</sub> production and decreased C<sub>1</sub>-C<sub>4</sub> gas products.

### 3. Conclusions

The effect of the cerium was investigated on the phase structure of nano-sized iron catalyst and the performance of the CO hydrogenation. Addition of Ce promoter into nano-sized iron catalysts increased CO conversion and chain growth probability to 74.6 % and 0.72 respectively and decreased

methane selectivity to 10.1 %. The changes in the catalytic performances can be attributed to the effect of promoter on H<sub>2</sub> and CO adsorption, which further significantly affects the FTS performances of the catalysts. In comparison to the unpromoted catalyst, the promoted iron catalyst considerably improved the FTS and WGS activities.

### Acknowledgements

We are grateful to the Research and Development of National Iranian Oil Company (NIOC) for financial support, which enabled this work to be undertaken. We also express our thanks to central laboratory of Ferdowsi University of Mashad for recording TEM micrographs.

### References

- Davis B.H., 2009, Fischer–Tropsch Synthesis: Reaction mechanisms for iron catalysts, *Catalysis Today* 141, 25-33.
- Anderson R.B., 1984, *The Fischer-Tropsch Synthesis*, Academic Press Inc, Orlando, Florida, USA.
- Van Der Laan G.P., Beenackers A.C.M., 2000, Intrinsic kinetics of the gas–solid Fischer–Tropsch and water gas shift reactions over a precipitated iron catalyst, *Applied Catalysis A: General* 193, 39–53.
- Bayat M, Rahmani F, Mazinani S, Rahimpour M R, 2010, Enhancement of Gasoline Production in a Novel Optimized Hydrogen-Permselective Membrane Fischer- Tropsch Reactor in GTL Technology; *Chemical Engineering Transactions*, 21, 1477-1482.
- Pour A.N., Housaindokht M.R., Zarkesh J., Irani M., Ganji E.B., 2012, Kinetics study of CO hydrogenation on a precipitated iron catalyst. *Journal of Industrial & Engineering Chemistry*, 18, 597-603.
- Pendyala V.R.R., Jacobs G., Mohandas J.C., Luo M., Ma W., Gnanamani M.K., Davis B.H., 2010. Fischer-Tropsch synthesis: Attempt to tune FTS and WGS by alkali promoting of iron catalysts, *Applied Catalysis A: General*, 389, 131-139.
- Bukur D.B., Mukesh D., Patel S.A., 1990, Promoter effects on precipitated iron catalysts for Fischer-Tropsch synthesis., *Industrial & Engineering Chemistry Research*, 29, 194 - 204.
- Luo M., O'Brien R.J., Bao S., Davis B.H., 2003, Fischer-Tropsch synthesis: induction and steady-state activity of high-alpha potassium promoted iron catalysts, *Applied Catalysis A: General*, 239, 111-120.
- Zhao L., Liu G., Li J., 2009, Effect of La<sub>2</sub>O<sub>3</sub> on a Precipitated Iron Catalyst for Fischer-Tropsch Synthesis, *Chinese Journal of Catalysis*, 30, 637-642.
- Feyzi M., Irandoust M., Mirzaei A.A., 2011, Effects of promoters and calcination conditions on the catalytic performance of iron-manganese catalysts for Fischer-Tropsch synthesis, *Fuel Processing Technology*, 92, 1136-1143.
- Palma V., Palo E., Castaldo F., Ciambelli P., Iaquaniello G., 2011. Catalytic activity of CeO<sub>2</sub> supported Pt-Ni and Pt-Co catalysts in the low temperature bio-ethanol steam reforming, *Chemical Engineering Transactions*, 25, 947-952.
- Suo H., Wang S., Zhang C., Xu J., Wu B., Yang Y., Xiang H., Li Y.W., 2012, Chemical and structural effects of silica in iron-based Fischer–Tropsch synthesis catalysts, *J. of Catalysis*, 286, 111-123.
- Pour A.N., Kamali Shahri S.M., Bozorgzadeh H.R., Zamani Y., Tavasoli A., Ahmadi M.M., 2008, Effect of Mg, La and Ca promoters on the structure and catalytic behavior of iron-based catalysts in Fischer–Tropsch synthesis, *Applied Catalysis A: General*, 348, 201-208.
- Zamani Y., Yousefian S.H., Pour A.N., Moshtari B., Bahadoran F., Taheri S.A., 2010, *Chemical Engineering Transactions*, 21, 1045- 1050.
- Herranz T., Rojas S., Perez-Alonso F.J., Ojeda M., Terreros P., Fierro J.L.G., 2006, CO<sub>2</sub> hydrogenation over promoted Fe-Mn catalysts prepared by the microemulsion methodology., *Applied Catalysis A: General*, 311, 66-75.
- Patterson A., 1939. The Scherrer Formula for X-Ray Particle Size Determination, *Physical Review*, 56, 978–982.
- Yang Y., Xiang H.W., Xu Y.Y., Bai L., Li Y.W., 2004, Potassium Effects on Activated-Carbon-Supported Iron Catalysts for Fischer–Tropsch Synthesis, *Appl. Catalysis A: General*, 266, 181-194.